AGU PUBLICATIONS

JGR

Journal of Geophysical Research: Oceans

RESEARCH ARTICLE

10.1002/2016JC011789

Key Points:
- Spectra for phytoplankton and nitrate are compared for the first time
- Different N-P spectral relationship found for length scale ranges 8–115 km and 10–100 m
- Results challenge extant theories of plankton patchiness

Correspondence to:
S. van Gennip,
s.van.gennip@noc.ac.uk

Citation:
van Gennip, S., A. P. Martin, M. A. Srokosz, J. T. Allen, R. Pidcock, S. C. Painter, and M. C. Stinchcombe (2016), Plankton patchiness investigated using simultaneous nitrate and chlorophyll observations, *J. Geophys. Res. Oceans*, *121*, 4149–4156, doi:10.1002/2016JC011789.

Received 11 MAR 2016
Accepted 11 MAY 2016
Accepted article online 17 MAY 2016
Published online 18 JUN 2016

Plankton patchiness investigated using simultaneous nitrate and chlorophyll observations

Simon van Gennip[1,2], Adrian P. Martin[1], Meric A. Srokosz[1], John T. Allen[3], Rosalind Pidcock[2], Stuart C. Painter[1], and Mark C. Stinchcombe[1]

[1]National Oceanography Centre, Southampton, UK, [2]Ocean and Earth Science, National Oceanography Centre, University of Southampton, Southampton, UK, [3]School of Earth and Environmental Sciences, Portsmouth, UK

Abstract The complex patterns observed in marine phytoplankton distributions arise from the interplay of biological and physical processes, but the nature of the balance remains uncertain centuries after the first observations. Previous observations have shown a consistent trend of decreasing variability with decreasing length scale. Influenced by similar scaling found for the properties of the water that the phytoplankton inhabit, "universal" theories have been proposed that simultaneously explain the variability seen from meters to hundreds of kilometers. However, data on the distribution of phytoplankton alone have proved insufficient to differentiate between the many causal mechanisms that have been suggested. Here we present novel observations from a cruise in the North Atlantic in which fluorescence (proxy for phytoplankton), nitrate, and temperature were measured simultaneously at scales from 10 m to 100 km for the first time in the open ocean. These show a change in spectra between the small scale (10–100 m) and the mesoscale (10–100 km) which is different for the three tracers. We discuss these observations in relation to the current theories for phytoplankton patchiness.

1. Introduction

Satellite images regularly show visually striking cases of phytoplankton patchiness, a phenomenon which may play a role in ecosystem stability [*Bracco et al.*, 2000; *Perruche et al.*, 2011] and phytoplankton diversity [*Károlyi et al.*, 2000; *Perruche et al.*, 2010]. Such heterogeneous spatial structures arise from the combined action of biological and physical processes, particularly at the mesoscale and submesoscale (1–500 km) where both act on similar timescales. The dominant physical processes at these scales are eddies and fronts, which continuously stir and mix the phytoplankton-bearing water to form convoluted filamentary structures. Concurrently, nonlinear biological interactions such as growth and mortality—in response to local changes in the availability of nutrients and light, and the effects of grazing by zooplankton—also modify phytoplankton distributions.

The power spectrum—which quantifies the amount of variability as a function of length scale—has proved a popular tool to describe phytoplankton spatial variability. Phytoplankton spectra typically have a power law relationship with inverse length scale, which corresponds to a straight line in log-log space [*Gower et al.*, 1980; *Mackas and Boyd*, 1979; *Martin and Srokosz*, 2002; *Platt*, 1972]. The slope of the logarithm of the spectrum, here denoted α, quantifies how spatial variability is distributed across length scales. For phytoplankton, observations suggest that it is invariably negative; the steeper the line, the less variability exists at smaller scales relative to larger ones.

Inspired by "universal" theories for the dynamics of physical turbulence, where a decreasing trend of variability with decreasing length scale is also seen, similar explanations have been put forward to explain phytoplankton patchiness as a balance between turbulent stirring by the water and biological processes involving the phytoplankton. There are four main such theories.

The first theory [*Denman and Platt*, 1976; *Denman et al.*, 1977] is based on the argument that the timescale associated with turbulent motion may decrease with length scale but the biological response time is invariant with scale. At small scales, where physical processes act fastest, the spectral slope of phytoplankton should be identical to that of physical variables such as temperature. In contrast, at longer length scales, the biological processes are quickest, and there is predicted to be a flattening of the phytoplankton spectral

slope relative to smaller scales that is not mirrored in physical variables. The second theory [*Hernández-García et al*., 2002] takes the notion of a single biological timescale further, arguing that it will be common to all interacting components of the planktonic ecosystem. A consequence is that all the ecosystem components—whether nutrients, phytoplankton, or zooplankton—are predicted to have identical power spectral slopes. In contrast, the third theory [*Bracco et al*., 2009] argues that the biological timescale is not a timescale associated with the response of the system as a whole; instead, it is defined as intrinsic to each constituent of the ecosystem and is determined by how quickly it responds to perturbation in its environment. Consequently, it is argued that ecosystem components with different reaction timescales should present spectra with differing slopes: the fastest reacting component displaying the steepest spectral slope. The fourth theory [*Lévy and Klein*, 2004] challenges the idea of a "cascade" of variability from large scales to small scales, a central tenet in the theories for physical turbulence which explain power law behavior [*Kolmogorov*, 1941; *Kraichnan*, 1974]. *Lévy and Klein* [2004] argue that although variability is still transferred between scales by stirring, the upwelling of nutrients at a range of intermediate scales, particularly within the mesoscale and submesoscale, injects extra variability. The response to such localized enhancement of phytoplankton growth is ephemeral and often significantly perturbs the ecosystem relative to background conditions. A consequence is that spectral slopes for different components of the ecosystem no longer need match [*Lévy and Klein*, 2004; *Lévy et al*., 2005].

Although numerous observations already exist for phytoplankton patchiness, they have proved very variable and do not allow us to distinguish between the above theories. In particular, interpretation of variability by comparing phytoplankton spectral slopes from different observations and model studies is made difficult by inconsistency in method [*Franks*, 2005; *van Gennip*, 2014]. Simultaneously examining another component of the ecosystem that strongly interacts with and moves like phytoplankton potentially provides a better way of discriminating between theories. Comparisons with zooplankton have been made [*Mackas and Boyd*, 1979; *Martin and Srokosz*, 2002; *Tsuda et al*., 1993] but the motile nature of zooplankton [*Folt and Burns*, 1999] makes a phytoplankton-zooplankton comparison unsuitable for testing the above theories which do not take the motility into account. Nutrients, however, are advected in an identical manner to phytoplankton by the ambient flow, and therefore a nutrient-phytoplankton comparison constitutes a more robust means of exploring the controls on phytoplankton patchiness in the context of existing theories. It is worth noting that no current theory predicts the cross correlation or phase between different components of the ecosystem. Hence, we can restrict our attention to the slopes of spectra even though doing so loses phase information [*Armi and Flament*, 1985].

Here we present results based on the first (to our knowledge) open ocean simultaneous continuous spatial measurements of phytoplankton and nitrate. Using this novel approach—of analyzing simultaneous nitrate, phytoplankton, and temperature spectra—we investigate key characteristics of phytoplankton patchiness, namely the consistency of spectral slope across scales and the shape of the spectrum if not of consistent slope. We then discuss the extent to which these results support existing theories.

2. Data

The data used are from *RRS Discovery* cruise D321 which took place between the 24 July and 23 August 2007 in the vicinity of Ocean Weather Station India (OWSI) (60°N 20°W). The survey area was populated by a number of mesoscale features, including a dipole, consisting of a cyclonic eddy and an anticyclonic mode-water eddy either side of a jet. The euphotic layer (∼64 m) was always deeper than the mixed layer depth (∼30m). Conditions were typical of late summer, post diatom bloom in the subpolar North Atlantic region with low silicate concentrations (0.52 mmol m^{-3}) and persisting nitrate (3.77 mmol m^{-3}) and phosphate (0.3 mmol m^{-3}) concentrations [*Forryan et al*., 2012]. The phytoplankton community was dominated by small flagellates with small proportions of diatoms, coccolithophores and Synechococcus [*Poulton et al*., 2010] and maximum rates of primary production occurred at the surface (5–20 m).

A ∼100 km square box was mapped, with parallel transects arranged in a radiator style running east-west. Sampling was done using SeaSoar, an undulating towed vehicle (Figure 1). Transects were ∼14 km apart and each one took ∼8 h to complete [*Pidcock et al*., 2013]. Due to weather conditions and SeaSoar mechanical problems, only two entire transects and two half transects were successfully sampled. SeaSoar was equipped with an SUV-6 fast response (1 Hz) UV nitrate sensor [*Pidcock et al*., 2010] and more standard

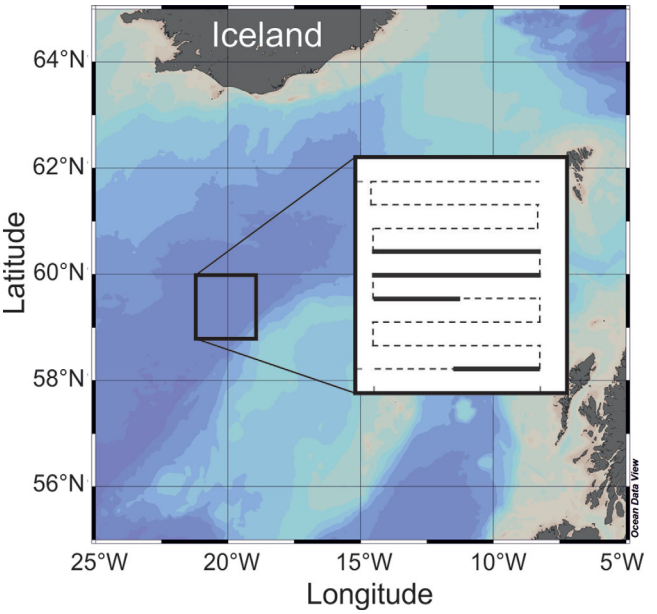

Figure 1. Area covered by the Seasoar survey. Solid lines in the inset image correspond to transect legs or parts of transect legs for which simultaneous nitrate and chlorophyll-*a* measurements are available and used for this study.

instruments such as a fluorometer and mini CTD for measuring chlorophyll fluorescence (hereafter chl-*a*) and temperature and salinity, respectively. This suite of instruments allowed nitrate measurements to be made simultaneously with chl-*a* and temperature. The undulations of SeaSoar traverse the top 400 m of the water column with a sampling rate of 1 Hz. Data points are approximately 4 m apart horizontally as a result of the ship's speed being held constant at 8 knots.

The data used for this study were extracted from the surface mixed layer where phytoplankton were most abundant. The mixed layer depth varied from 30 to 50 m. Data were used from the depth range 15–25 m to avoid quenching effects on near surface chl-*a* observations. A few profiles showed a significant increase in density with depth within this depth range. For these, only data shallower than the point of increase were used.

Two ranges of length scales are investigated in this study. Data at the small scale (10–100 m) comprise clusters of 1 Hz observations as SeaSoar traverses the 15–25 m depth range on each ascent and descent. Because observations are separated by ∼4 m horizontally, no structure smaller than 8 m can be resolved. The largest scale resolved in this range (100 m) is set by the time taken for SeaSoar to traverse the depth range. Data at the larger spatial scale (8–115 km) arise from taking the mean value of each of the above clusters. One full undulation of SeaSoar took place approximately every 3.5 km, and so the larger scale data

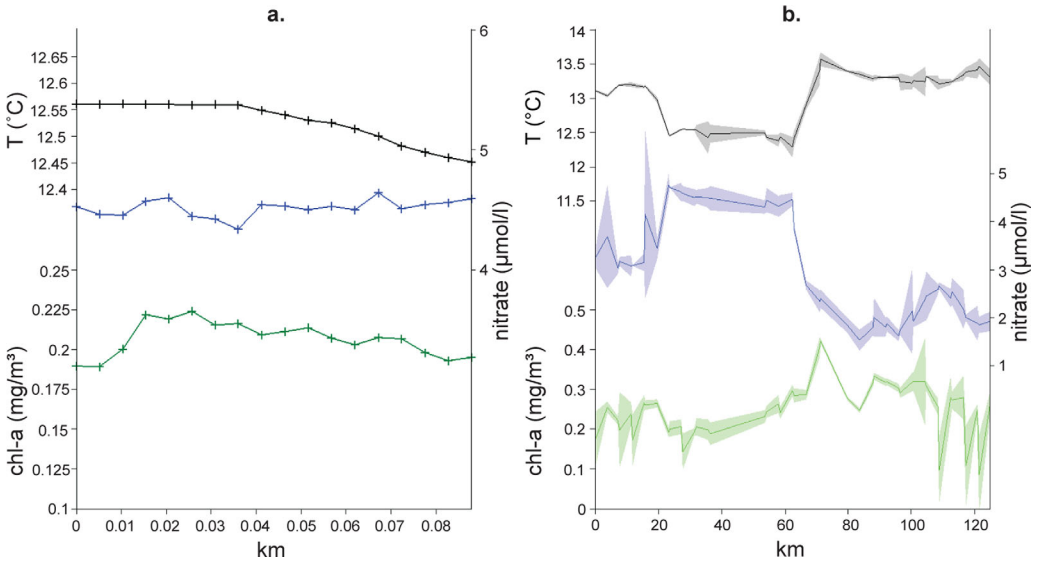

Figure 2. Measurements within depth range 15–25 m for temperature T (black), nitrate (blue), and chlorophyll-*a* Chl-*a* (green) obtained along a transect. (a) An example of a series of measurements, collected by the sampling vehicle from one passage through the depth range 15–25 m, used for spectrum estimation for the range 10–100 m. (b) Data points—corresponding to mean values from each ascent/descent of the vehicle through the depth range—used for spectrum calculation for the range 8–115 km. Error bars (shaded) correspond to two standard deviations either side of the mean.

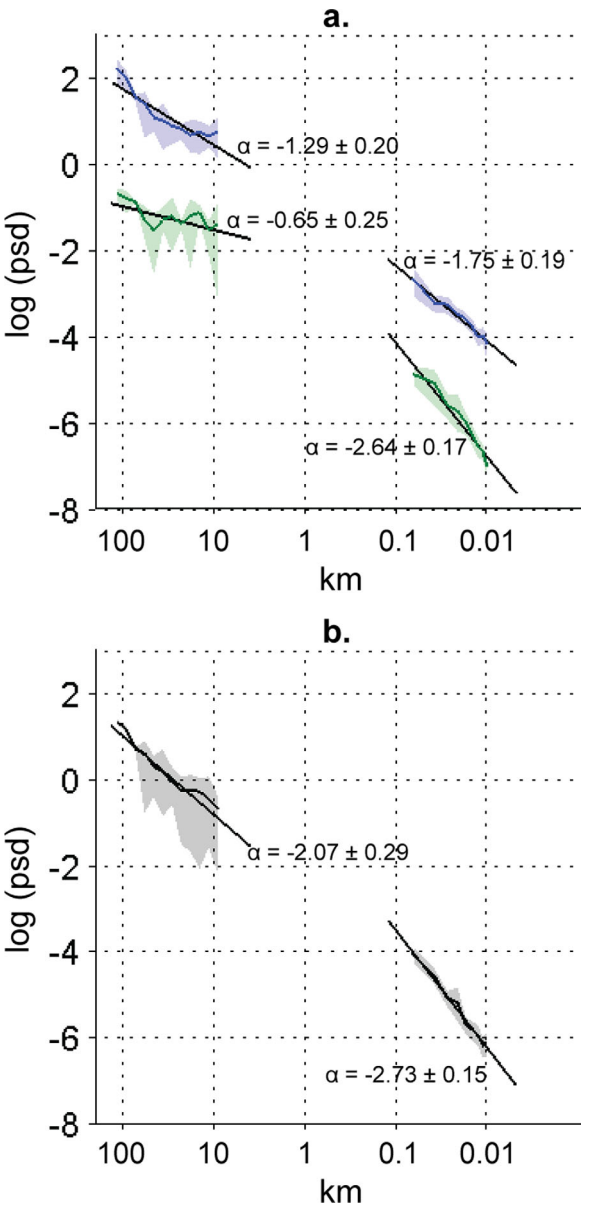

Figure 3. Power spectral density estimates (psd) based on all four SeaSoar transect sections: (a) nitrate (blue) and chlorophyll-*a* (green), (b) temperature. Lines, uncertainty in slope, and 95% confidence intervals (shaded), are obtained using parameters estimated using bootstrapping. Note the absence of estimates within the 0.1–8 km range due to the sampling strategy.

set cannot resolve structures smaller than ~8 km. The upper limit of resolution (~115 km) is set by the length of transects. The nature of the sampling meant that no spatial information could be collected for the range 100 m to 8 km. Examples of nitrate, chl-*a* and temperature variability over both ranges of scales are displayed in Figure 2.

3. Methods

Spatial variability spectra were estimated for nitrate, chlorophyll-*a*, and temperature. The different sampling characteristics at small and large scales require different approaches to be taken for the analysis.

At small scales (10–100 m), the traditional Fast Fourier Transform (FFT) was used. The regularity of intervals between data points in each cluster, a prerequisite for the application of FFT, was provided by the constant speed of the ship. Data were additionally "whitened" using a first-order difference to minimize leakage in the spectral estimates [*Jenkins and Watts*, 1968]. The effect of prewhitening was then removed by "post-colouring" the spectral estimates. The power spectrum of each variable was obtained by grouping the power estimates derived from all cluster groups into wavelength bins of equal width, followed by averaging [*Bendat and Piersol*, 1971].

At larger scales, spectral estimates were obtained using the Lomb-Scargle periodogram method [*Press et al.*, 2007]. This technique was used because of the irregular spacing of the data points resulting from the occasionally uneven nature of the SeaSoar's undulations. An advantage of this method is that the wavelengths for which the spectral power is estimated can be chosen. Consequently power estimates for all transects could be calculated for a common set of predefined wavelengths. Such a method also avoids the need to group estimates prior to averaging. A set of wavelengths was chosen so that their logarithms were evenly spaced in log space. After visually checking for power law behavior for each transect (linear in log-log space), the spectrum for each variable was obtained by averaging the power over all four transects for each wavelength investigated.

The slope of each spectrum was obtained by applying a linear regression to the log-averaged power estimates against the log of wavelength (slope in log-log space being equivalent to the power law exponent). To give more robust results, a single regression was done for each scale range, pooling data from all transects for the larger scales (8–115 km), and from all clusters for the smaller scales (10–100 m).

Distributions for each slope estimate were obtained by performing regressions on 10,000 data subsets generated from the full spectrum using a bootstrap routine, randomly selecting 90% of spectral estimates with

Table 1. (a) Spectral Slope for Nitrate, Temperature and chl-*a*, with Their Respective *r* Value and Standard Deviation and (b) Statistical Properties for the Distribution of the Slope Difference Between Two Variables: Mean and Standard Deviations[a]

		Range 8–115 km			Range 10–100 m		
	Variable	Slope (α)	Standard dev.	*r*	Slope	Standard dev.	*r*
a	Nitrate	−1.29	0.20	−0.85	−1.75	0.19	−0.96
	Chl-*a*	−0.65	0.25	−0.54	−2.64	0.17	−0.96
	Temperature	−2.07	0.29	−0.89	−2.73	0.15	−0.98
		Slope difference			Slope difference		
b	Nitrate-Chl-*a*	−0.64	0.27		0.90	0.25	
	Nitrate-Temperature	0.78	0.32		0.99	0.22	
	Chl-*a*-Temperature	1.42	0.21		0.09	0.22	

[a]Distributions were obtained from 10,000 data sets generated using a bootstrap routine with 90% randomly selected spectral estimates with replacement. The *r*-value is obtained from fitting a regression line to the mean spectral estimates against the inverse of length scale in log-log space.

replacement. For each random subset generated, slopes for each variable were estimated following the procedures described above. The 95% confidence intervals displayed in Figure 3 at each wavelength were obtained by retrieving the 2.5 and 97.5 percentiles from the distribution of each spectral estimate. Results were unaffected when increasing the number of bootstrap generated data subsets. The uncertainty in the slope estimates (see Table 1) was quantified by the standard deviation of the above distributions. Analysis of the difference between spectral slopes followed a similar procedure, in this case using bootstrapping to generate a distribution for the difference between two variables' spectral slopes.

4. Results

The spectra and respective slopes for both spatial scales are displayed in Figure 3. Both nitrate and chl-*a* display a similar spectral shape, often described as a "knee" [*Steele*, 1978] when plotted on a logarithmic scale, which is characteristic of a shift in power law behavior. This shift is less pronounced for the nitrate spectrum ($\alpha = -1.29$ for scales 8–115 km; $\alpha = -1.75$ for scales 10–100 m) than for phytoplankton ($\alpha = -0.65$ for 8–115 km; $\alpha = -2.64$ for 10–100 m).

For both length-scale ranges, the spectral slopes of nitrate and chl-*a* are different. For the range 8–115 km, this difference in slopes is significant at the 95% confidence level with a mean difference of −0.64. For the range 10–100 m, it is significant at the 99% confidence level with a mean difference of 0.90 (Table 1).

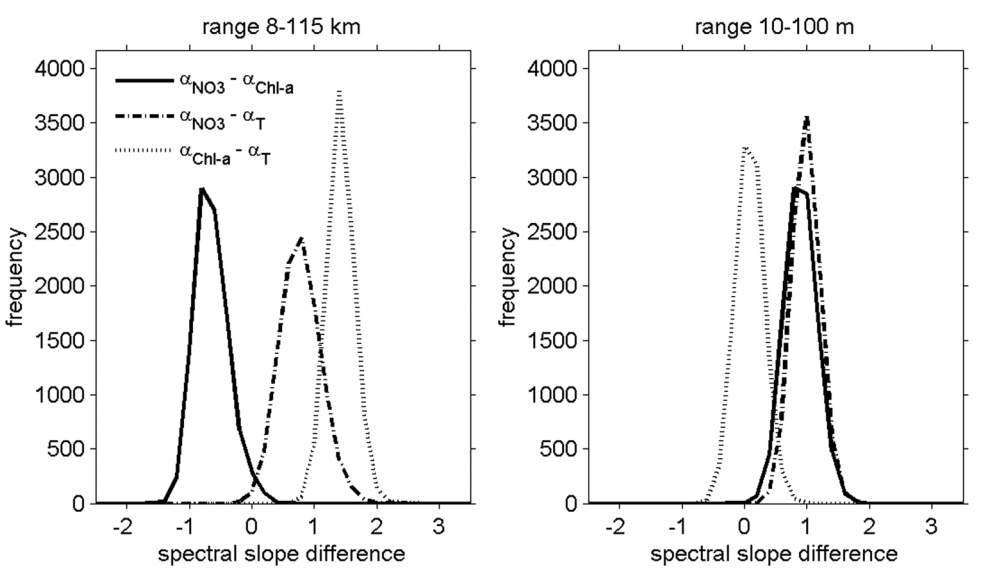

Figure 4. Distribution of the difference in spectral slope between nitrate (NO_3) and chlorophyll-*a* (solid line), nitrate and temperature (dashed), and chlorophyll-*a* and temperature (dotted) for the range 8–115 km (left) and the range 10–100 m (right).

From Figure 3, it can be seen that slopes of both nitrate and phytoplankton are different to that of temperature ($\alpha = -2.07$) for the range 8–115 km. Differences in slope are significant at the 99% confidence level (Figure 4): nitrate and temperature, with mean difference 0.78; phytoplankton and temperature with mean difference 1.48. This is not the case for the range 10–100 m: nitrate ($\alpha = -1.75$) and temperature ($\alpha = -2.73$) differ significantly at the 99% confidence level (mean difference of 0.99 and standard deviation of 0.22). However, at these smaller scales, the difference in slopes for chl-*a* ($\alpha = -2.64$) and temperature—with mean difference of 0.09 and standard deviation of 0.22—is not statistically significant.

As an extra check on the influence of potential quenching effects on the fluorescence signal, the analysis was repeated using only night time data. The results are unchanged at scales of 10–100 m. The only significant impact is greater uncertainty in spectral slopes in the range 8–115 km. This is inevitable given the small data set but does not affect our conclusions. No data from other depths were studied due to the relatively shallow mixed layer.

5. Discussion

5.1. Comparison to Models and Theory

The data set studied here is limited: from just one location, at just one time. Nevertheless, the simultaneous measurement of temperature, chl-*a*, and, particularly, nitrate over multiple scales provides an informative new perspective on the processes responsible for phytoplankton patchiness.

The presence of a "knee" in the spectra, rather than a constant scaling across all scales, has been observed previously [*Denman and Platt*, 1976; *Denman et al*., 1977; *Lovejoy et al*., 2001]. New insight is provided by the difference in spectral slopes either side of this knee, whether comparing nitrate and phytoplankton or nitrate and temperature. The spectral slopes for temperature and phytoplankton at the small scales are not significantly different whereas they differ at the larger scales (phytoplankton flatter than temperature). The behavior of these two tracers seems, therefore, to be consistent with a theory of shorter physical timescales setting the spectra of both tracers at small spatial scales and shorter biological ones flattening that for phytoplankton at larger ones [*Denman and Platt*, 1976]. However, the nitrate spectral slope differs from those of phytoplankton and temperature both sides of the knee. This raises the question of whether nitrate and phytoplankton are responding to forcing with different timescales. Theoretical arguments imply that the spectral slopes for nitrate and phytoplankton should match if they have the same timescale of response [*Hernández-García et al*., 2002]. This theory was developed for the case of two-dimensional turbulence, analogous to the range of larger scales that we study. However, as the theoretical basis for a common timescale (based on a perturbation analysis of the ecosystem independent of the physical setting) is independent of the spatial scale, the argument could be extended to smaller scales. Regardless, we find the slopes for nitrate and phytoplankton to differ for both length ranges. *Hernández-García et al*. [2002] do discuss a scenario in which this can arise, where phytoplankton growth has no impact on its resource. Although it is true that nitrate concentrations are not limiting in our study, what is taken up by phytoplankton is lost from the nitrate pool so a direct coupling still exists, ruling out this particular scenario. If we take the different slopes as evidence that nitrate and phytoplankton have different timescales, then the comparison of their spectral slopes provides another constraint: for scales of 8–115 km the nitrate slope is steeper and the reverse is true for 10–100 m. Although they did not model nitrate, *Bracco et al*. [2009] demonstrated that allowing different components of the ecosystem (there phytoplankton and an idealized nonmotile zooplankton) to have different timescales of response did allow them to exhibit different spectral slopes. In the context of our results, this leaves the question once again of why the timescale would be different either side of the knee.

An alternative is that variability is being injected at scales between 100 m and 8 km. This range of scales has been termed the submesoscale. There is considerable evidence to suggest that physical processes significantly impact the ecosystem at these scales [e.g., *Mahadevan*, 2016]. Use of a model of high enough spatial resolution to capture some of these submesoscale dynamics [*Lévy and Klein*, 2004] shows that the relative spectral slopes of components of the ecosystem can vary independently due to short-lived localized upwelling.

Our observations appear consistent with these model results, so it may be that the intermittent forcing at the submesoscale (1–10 km) [*Callies and Ferrari*, 2013], allows the relative slope for nitrate relative to phytoplankton to take different values either side of this range. The mechanism leading to the different relative

slopes for nitrate and phytoplankton remains unknown. In the *Lévy and Klein* [2004] study, the relative slopes were also found to vary with time. This might be an indication that the difference in slopes may be related to different transient responses to the perturbations introduced by localized upwelling. Time series of spectra must therefore be a priority.

Another modeling study [*Smith et al*., 2016] on the effects of submesoscale turbulence on nonreactive, passive, ocean tracers gives further support for this influence of submesoscale forcing. *Smith et al*. [2016] show a change in spectral slope between the small scale (5–100 m) and submesoscale (1–20 km), with slopes in the submesoscale range being somewhat steeper (their Figure 10), for tracers relevant to the problem of plankton patchiness. Their small scale slope estimates for nonreactive passive tracers (−2.25 to −2.4; their Figure 10) are of a similar order to that found here for chl-*a* (−2.64), but differ from that for nitrate (−1.75). They state that the spectra have peaks associated with physical processes at their characteristic submesoscale length scale of 5 km and the Langmuir length scale of 10 m (though the existence of the latter is not clear from their Figure 10). In relation to our results, the predicted submesoscale peak at 5 km lies within the spectral gap of the observations. Their other spectral peak at the Langmuir scale of 10 m is at the limit of our small-scale spectral estimates, so again direct comparison is problematic. It is possible that spectral peaks could exist at these length scales but our observations do not provide data at these scales. Therefore, our struggle to understand plankton patchiness would be well-served by focusing future observations on the length scales 1–10 km and below 10 m.

5.2. Parameterizing Subgrid-Scale Variability in Models

The benefit of consistent power law spectral behavior would be that variability at one scale could be estimated from observations at a different scale in a straightforward manner. Current global climate models that reproduce marine biogeochemistry fail to adequately represent phytoplankton dynamics beyond the mesoscale: effects at smaller scales are quantified by using spatial and temporal averages over a grid-cell scale. A power law scaling in ecosystem variables could potentially provide a basis for parameterizations that implicitly capture phytoplankton dynamics at subgrid scale. Such a principle has already been successfully implemented in global circulation models to resolve subgrid-scale physical processes affecting mixed layer stratification [*Fox-Kemper and Ferrari*, 2008; *Fox-Kemper et al*., 2008, 2011]. By analogy, bearing in mind the potential importance of the mesoscale and submesoscale for ocean primary production [*Lévy et al*., 2012], in theory, such an approach for a description of phytoplankton behavior could present the opportunity to improve model predictions for a relatively small computational cost. However, evidence of a change in power law behavior at a critical scale within the submesoscale, together with variations in the spectral relationship between ecosystem components makes such an endeavor challenging and one for which we currently have insufficient information.

6. Conclusions

In this study, we have analyzed spectra for phytoplankton and nitrate simultaneously for the first time, based on novel measurements made in the North Atlantic. More specifically, we compared the slopes of their power spectra over the ranges (10–100 m) and (8–115 km). Significant differences in spectral slopes between chlorophyll-*a* and nitrate were found between ranges, giving their spectra a shape previously referred to as a "knee." Most notably it was found that their relative slope changes for both small scales (10–100 m) and the mesoscale (8–115 km). The observed spectral behavior is consistent with that seen in models with intermittent localized upwelling, particularly at the submesoscale. Our results suggest that future observations should focus on filling the spectral gap in the submesoscale range O(1–10 km) and at Langmuir scales O(10 m and below) where there may be injection of nutrients [*Smith et al*., 2016]. It is also important to collect time series of spectra given the possibility that the relative slopes may be changing with time [cf. *Lévy and Klein*, 2004]. Characterizing and explaining plankton patchiness continues to be a challenging oceanographic problem despite its venerable age, the first observations having been made centuries ago.

Acknowledgments
The fieldwork was funded by the Natural Environment Research Council through the Oceans 2025 research programme and NERC National Capability funding. S. van Gennip thanks NERC and University of Southampton for his studentship funding. Data used in this study are available through the British Oceanographic Data Centre (http://www.bodc.ac.uk/).

References

Armi, L., and P. Flament (1985), Cautionary remarks on the spectral interpretation of turbulent flows, *J. Geophys. Res.*, *90*(C6), 11,779–11,782.

Bendat, J. S., and A. G. Piersol (1971), *Random Data: Analysis and Measurement Procedures*, John Wiley & Sons, Inc., Hoboken, N. J.

Bracco, A., A. Provenzale, and I. Scheuring (2000), Mesoscale vortices and the paradox of the plankton, *Proc. R. Soc. London, Ser. B*, *267*(1454), 1795–1800.
Bracco, A., S. Clayton, and C. Pasquero (2009), Horizontal advection, diffusion, and plankton spectra at the sea surface, *J. Geophys. Res.*, *114*, C02001, doi:10.1029/2007JC004671.
Callies, J., and R. Ferrari (2013), Interpreting energy and tracer spectra of upper-ocean turbulence in the submesoscale range (1–200 km), *J. Phys. Oceanogr.*, *43*(11), 2456–2474.
Denman, K. L., and T. Platt (1976), The variance spectrum of phytoplankton in a turbulent ocean, *J. Mar. Res.*, *34*(4), 593–601.
Denman, K. L., A. Okubo, and T. Platt (1977), Chlorophyll fluctuation spectrum in sea, *Limnol. Oceanogr.*, *22*(6), 1033–1038.
Folt, C. L., and C. W. Burns (1999), Biological drivers of zooplankton patchiness, *Trends Ecol. Evol.*, *14*(8), 300–305.
Forryan, A., A. P. Martin, M. A. Srokosz, E. E. Popova, S. C. Painter, and M. C. Stinchcombe (2012), Turbulent nutrient fluxes in the Iceland Basin, *Deep Sea Res., Part I*, *63*, 20–35.
Fox-Kemper, B., and R. Ferrari (2008), Parameterization of mixed layer eddies. Part II: Prognosis and impact, *J. Phys. Oceanogr.*, *38*(6), 1166–1179.
Fox-Kemper, B., R. Ferrari, and R. Hallberg (2008), Parameterization of mixed layer eddies. Part I: Theory and diagnosis, *J. Phys. Oceanogr.*, *38*(6), 1145–1165.
Fox-Kemper, B., G. Danabasoglu, R. Ferrari, S. M. Griffies, R. W. Hallberg, M. M. Holland, M. E. Maltrud, S. Peacock, and B. L. Samuels (2011), Parameterization of mixed layer eddies. III: Implementation and impact in global ocean climate simulations, *Ocean Modell.*, *39*(1–2), 61–78.
Franks, P. J. S. (2005), Plankton patchiness, turbulent transport and spatial spectra, *Mar. Ecol. Progr. Ser.*, *294*, 295–309.
Gower, J. F. R., K. L. Denman, and R. J. Holyer (1980), Phytoplankton patchiness indicates the fluctuation spectrum of mesoscale oceanic structure, *Nature*, *288*(5787), 157–159.
Hernández-García, E., C. López, and Z. Neufeld (2002), Small-scale structure of nonlinearly interacting species advected by chaotic flows, *Chaos*, *12*(2), 470–480.
Jenkins, G. M., and D. G. Watts (1968), *Spectral Analysis and Its Applications*, Holden-Day, Oakland, Calif.
Károlyi, G., Á. Péntek, I. Scheuring, T. Tél, and Z. Toroczkai (2000), Chaotic flow: The physics of species coexistence, *Proc. Natl. Acad. Sci. U. S. A.*, *97*(25), 13,661–13,665.
Kolmogorov, A. N. (1941), The local structure of turbulence in incompressible viscous fluid for very large reynolds numbers, *Dokl. Akad. Nauk SSSR*, *30*, 301–305.
Kraichnan, R. H. (1974), Convection of a passive scalar by a quasi-uniform random straining field, *J. Fluid Mech.*, *64*(4), 737–762.
Lévy, M., and P. Klein (2004), Does the low frequency variability of mesoscale dynamics explain a part of the phytoplankton and zooplankton spectral variability?, *Proc. R. Soc. London, Ser. A*, *460*(2046), 1673–1687.
Lévy, M., M. Gavart, L. Mémery, G. Caniaux, and A. Paci (2005), A 4D-mesoscale map of the spring bloom in the northeast Atlantic (POMME experiment): Results of a prognostic model, *J. Geophys. Res.*, *110*, C07S10, doi:10.1029/2004JC002588.
Lévy, M., D. Iovino, L. Resplandy, P. Klein, G. Madec, A. M. Tréguier, S. Masson, and K. Takahashi (2012), Large-scale impacts of submesoscale dynamics on phytoplankton: Local and remote effects, *Ocean Modell.*, *43–44*, 77–93.
Lovejoy, S., W. J. S. Currie, Y. Tessier, M. R. Claereboudt, E. Bourget, J. C. Roff, and D. Schertzer (2001), Universal multifractals and ocean patchiness: Phytoplankton, physical fields and coastal heterogeneity, *J. Plankton Res.*, *23*(2), 117–141.
Mackas, D. L., and C. M. Boyd (1979), Spectral analysis of zooplankton spatial heterogeneity, *Science*, *204*(4388), 62–64.
Mahadevan, A. (2016), The impact of submesoscale physics on primary productivity of plankton, *Annu. Rev. Mar. Sci.*, *8*(1), 161–184.
Martin, A. P., and M. A. Srokosz (2002), Plankton distribution spectra: Inter-size class variability and the relative slopes for phytoplankton and zooplankton, *Geophys. Res. Lett.*, *29*(24), 2213, doi:10.1029/2002GL015117.
Perruche, C., P. Rivière, P. Pondaven, and X. Carton (2010), Phytoplankton competition and coexistence: Intrinsic ecosystem dynamics and impact of vertical mixing, *J. Mar. Syst.*, *81*(1–2), 99–111.
Perruche, C., P. Rivière, G. Lapeyre, X. Carton, and P. Pondaven (2011), Effects of surface quasi-geostrophic turbulence on phytoplankton competition and coexistence, *J. Mar. Res.*, *69*(1), 105–135.
Pidcock, R., M. Srokosz, J. Allen, M. Hartman, S. Painter, M. Mowlem, D. Hydes, and A. P. Martin (2010), A novel integration of an ultraviolet nitrate sensor on board a towed vehicle for mapping open-ocean submesoscale nitrate variability, *J. Atmos. Oceanic Technol.*, *27*(8), 1410–1416.
Pidcock, R., A. P. Martin, J. Allen, S. C. Painter, and D. Smeed (2013), The spatial variability of vertical velocity in an Iceland basin eddy dipole, *Deep Sea Res., Part I*, *72*, 121–140.
Platt, T. (1972), Local phytoplankton abundance and turbulence, *Deep Sea Res. Oceanogr. Abstr.*, *19*(3), 183–187.
Poulton, A. J., A. Charalampopoulou, J. R. Young, G. A. Tarran, M. I. Lucas, and G. D. Quartlya (2010), Coccolithophore dynamics in non-bloom conditions during late summer in the central Iceland Basin (July–August 2007), *Limnol. Oceanogr.*, *55*(4), 1601–1613.
Press, W. H., S. A. Teukolky, W. T. Vetterling, and B. P. Flannery (2007), *Numerical Recipes: The Art of Scientific Computing*, Cambridge Univ. Press, Cambridge.
Smith, K. M., P. E. Hamlington, and B. Fox-Kemper (2016), Effects of submesoscale turbulence on ocean tracers, *J. Geophys. Res. Oceans*, *121*, 908–933, doi:10.1002/2015JC011089.
Steele, J. H. (1978), *Spatial Pattern in Plankton Communities*, Springer Science+Business Media, Plenum Press, N. Y., doi:10.1007/978-1-4899-2195-6.
Tsuda, A., H. Sugisaki, T. Ishimaru, T. Saino, and T. Sato (1993), White-noise-like distribution of the oceanic copepod Neocalanus cristatus in the subarctic North Pacific, *Mar. Ecol. Prog. Ser.*, *97*(1), 39–46.
van Gennip, S. J. (2014), Understanding the extent of universality in phytoplankton spatial properties, Doctoral thesis, 176 pp., Univ. of Southampton, PhD. thesis.